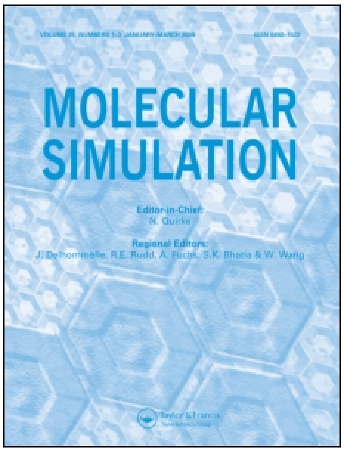

Molecular Simulation
Publication details, including instructions for authors and subscription information:
http://www.informaworld.com/smpp/title~content=t713644482

A theoretical study of the interactions of water with gallic acid and a PEO/TGG complex

R. Gaudreault[abc]; T. G. M. van de Ven[ab]; M. A. Whitehead[c]
[a] Department of Chemistry, McGill University, Montreal, Que., Canada [b] Pulp and Paper Research Centre, McGill University, Montreal, Que., Canada [c] Cascades Canada Inc., Recherche et Développement, Kingsey Falls, Que., Canada

To cite this Article Gaudreault, R. , van de Ven, T. G. M. and Whitehead, M. A.(2006) 'A theoretical study of the interactions of water with gallic acid and a PEO/TGG complex', Molecular Simulation, 32: 1, 17 — 27

To link to this Article: DOI: 10.1080/08927020500492047

URL: http://dx.doi.org/10.1080/08927020500492047

Molecular Simulation, Vol. 32, No. 1, 15 January 2006, 17–27

Taylor & Francis
Taylor & Francis Group

A theoretical study of the interactions of water with gallic acid and a PEO/TGG complex

R. GAUDREAULT[†‡¶]*, T. G. M. VAN DE VEN[†‡§] and M. A. WHITEHEAD[†||]

†Department of Chemistry, McGill University, 801 Sherbrooke Street West, Montreal, Que., Canada, H3A 2K6
‡Pulp and Paper Research Centre, McGill University, 3420 University Street, Montreal, Que., Canada, H3A 2A7
¶Cascades Canada Inc., Recherche et Développement, 471 Marie-Victorin Boul., Kingsey Falls, Que., Canada J0A 1B0

(Received August 2005; in final form November 2005)

PM3 Semi-empirical molecular orbital calculations on the interaction of water and gallic acid (GA) show the hydrophilic part of the solute (GA) to form strong directional bonds to 5 H_2O molecules. To form a monolayer around GA, containing trigalloyl glucose both hydrophilic and hydrophobic regions, requires about 43 H_2O molecules. PM3, MM and MD calculations on complexes between the hexamer of poly(ethylene oxide) $(PEO)_6$ and cofactor containing trigalloyl glucose (TGG) show that $(PEO)_6$/TGG complexes do not form in aqueous solution, which agrees with the experimental results in pure water, in the absence of salt, obtained with PEO and corilagin, a very similar molecule.

It is possible that a (PEO) conformers, with the oxygens outside, are favoured in aqueous solution, because the H_2O molecules can more easily hydrogen bond with the PEO ether oxygens.

A distinct change in the rate of change of the relative total energy per H_2O molecule occurs at 10 H_2O molecules: beyond 10 H_2O molecules a slow varying plateau is observed to and beyond 120 H_2O molecules. This is critical when calculating the enthalpy of association of a solvated molecular complex.

Keywords: Molecular simulation; Poly(ethylene oxide); Cofactor; Complex; Solvation

1. Introduction

The formation of a complex between poly(ethylene oxide) (PEO) and a cofactor has been considered necessary to flocculate cellulose fibres, fines and fillers, and to aid retention and drainage in papermaking. The high flocculation efficiency was assigned to several mechanisms [1–7]. Cofactors and PEO/cofactor interactions in the gas phase were studied using PM3 semiempirical molecular orbital theory [8,9], and molecular mechanics (MM) [10,11]; as yet there is no theoretical study of the solvated PEO/cofactor systems, which would be more relevant to pulp and paper applications. Therefore, solvation of the PEO/cofactor complexes is considered. Two models are commonly used to describe solvation: (i) the implicit model [12,13], which uses a bulk dielectric constant to reproduce the effect of the solvent on the solute and (ii) the explicit model [14,15], which takes into account the properties of each solvent molecule. The study of direct interactions between the hydrophilic part of a molecule and H_2O molecules, requires the solvent to be represented with an explicit solvent model [14,15]. The explicit model ensures that the electronic exchange between the solute and each water molecule is calculated explicitly [15,16].

Entropy plays a dominant role in nonbonding interactions and its change accompanying complex formation is always negative [17]. When two polymers associate their respective conformations will change. Enthalpy and entropy changes also reflect the changes in the interaction of polymer segments, with themselves, and with solvent molecules [18]. The hydration entropies of neutral solutes have been shown to be proportional to the solute surface area [19–21]. The potential energy scans (PES) of flexible PEO/cofactor complexes show a large number of enthalpically similar conformations with similar entropy changes. When the PEO/cofactor complex is solvated, a very complicated 3D search is required, giving many close enthalpy minima. The number of enthalpy minima increases rapidly with the complex size,

---

*Corresponding author. Tel.: + 1 819 363 5701. Fax: + 1 819 363 5755. Email: rgaudreault@cascades.com
§Tel.: + 1 514 398 6177. Fax: + 1 514 398 8254. Email: theo.vandeven@mcgill.ca
||Tel.: + 1 514 398 6239. Fax: + 1 514 398 3797. Email: tony.whitehead@mcgill.ca

Molecular Simulation
ISSN 0892-7022 print/ISSN 1029-0435 online © 2006 Taylor & Francis
http://www.tandf.co.uk/journals
DOI: 10.1080/08927020500492047

and the number of H_2O molecules, giving different entropy contributions.

Different types of valence bond theory interactions are possible in PEO/cofactor complexes: (i) Any $X-H\cdots A$ interaction is called a "hydrogen bond", if (a) it constitutes a local bond and (b) X–H acts as proton donor to A [22]. Hydrogen bonds are inherently directional, with linear or close to linear geometries favoured energetically over bent ones [23]; (ii) In contrast, van der Waals interactions are isotropic with interaction energies independent of the binding angle [23].

The concept of the H-bond has been extended to $CH\cdots Y$ bonding [17,23,24]. Theoretical calculations for weakly polarized C–H groups, estimate $CH\cdots O$ hydrogen bond energies to be in the range -0.5 to $-1\,\mathrm{kcal\,mol^{-1}}$ [23,25,26]. Recent molecular orbital PM3 calculations of the electron density map, showed the $R-OH\cdots O$ and $R-CH\cdots O$ interactions for the PEO/corilagin–boat complex, to range from 0.0205 to $0.0341\,\mathrm{e\,au^{-3}}$. An electron density of $0.0205\,\mathrm{e\,au^{-3}}$ for $R-CH\cdots O$ inter-molecular interactions between PEO and an oxygen of the glucopyranose ring of corilagin was found [9].

A dihydrogen bond $M-N\cdots H-Y$ was originally reported by Lee *et al.* [27] in metal complexes (M = metal element) as a $N-H\cdots H-B$. A neutron diffraction of the crystal H_3BNH_3 dimer showed the $H\cdots H$ distance to be short, about 1.7–2.2 Å [28]. In the PEO/cofactor complexes, the $R-OH\cdots H$ and $R-CH\cdots H$ distances were 1.73 and 1.71–1.76 Å [9]. The $R-CH\cdots H$ interactions [9] were found to be destabilizing with electron densities ranging from 0.0114 to 0.0130 [9].

The existence of an anti-hydrogen bond, $CH\cdots\pi$, was suggested by theory [29] and confirmed experimentally [30], and an $OH\cdots\pi$ interaction was included in the stabilization of a peptide–gallic acid complex [31] by theory. Using quantum simulation methods, Benoit *et al.* [32] showed the existence of a π-hydrogen bonded structure for phenol–$(H_2O)_n$, with ($n = 2$–5) hydrogen bonded clusters. No entropy effects were reported. *Ab initio* calculations, MP2/6–311++G(d,p), on phenol–water, gave a binding energy of $-2.57\,\mathrm{kcal\,mol^{-1}}$ for the hydrogen bonded phenol–H_2O [33]. An experimental binding energy of $-5.6 \pm 0.11\,\mathrm{kcal\,mol^{-1}}$ was reported for the gas phase π-hydrogen bonded phenol–H_2O neutral complex [34].

Hydrophobic interactions describe the association of nonpolar groups in aqueous solution. The association does not significantly change the enthalpy, because ΔH is close to zero, and consequently the process of association of nonpolar groups is governed by entropy [17]. Association is always connected with a negative entropy change, related to the ordering of molecules that surround the hydrocarbon parts of the original conformation [17]. In agreement with experiment, the theoretical hydration entropies are large and negative at room temperature [35]. A dominant factor in hydrophobic hydration is the formation of a cavity of water (solvent) molecules of a size and shape to accommodate a given solute molecule [16,35].

In the present work, GA and 1,3,6-Tri-*O*-galloyl-β-D-glucose (TGG), are studied because they are model PEO cofactors (figure 1). GA has been theoretically [31] and experimentally [36,37] studied, and TGG has been previously discussed [8,9]. GA, the solute used in the first part of the present paper, is a sub-group of the larger TGG cofactor; GA possesses hydrophilic and hydrophobic groups. Initially, $GA\cdot(H_2O)_n$ is used to study the effect on solvent which causes a change in the hydration enthalpy ΔH, entropy ΔS and free energy ΔG. Secondly, a larger complex $(PEO)_6$/TGG is used to study the effect of water

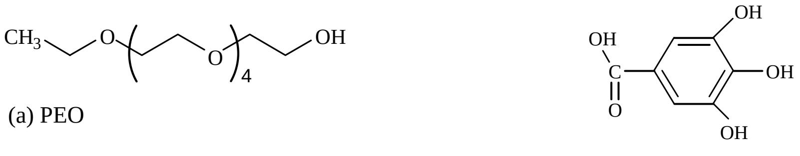

(a) PEO

(b) Gallic acid

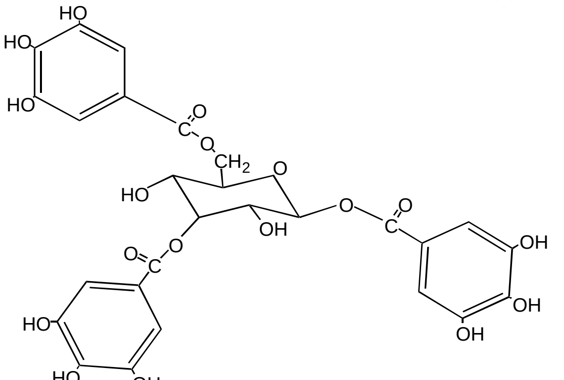

(c) TGG

Figure 1. Molecular structures of: (a) PEO hexamer; (b) Gallic acid (GA) [31] and (c) TGG [8].

on the enthalpy of association between PEO/TGG, and the conformational changes in the $(PEO)_6/TGG/(H_2O)_n$ complexes.

2. Conformational analysis

2.1 The programmes

Theoretical calculations used the Gaussian [38] GW03 Revision B.02 and the GaussViewW Version 3.07. The PM3 [39,40] semi-empirical calculations were performed using the methods described earlier [8,9]. All the theoretical results were obtained at 0 K; the correction to 298.15 K was made using a scaling factor of 0.9761 [41] to give theoretical results at 298 K which are obviously more suitable to compare with the experimental conditions in the pulp and paper industry.

2.2 The cofactors

The methods used to build the cofactors have been described [8]. The most stable TGG molecule has a tripod shape, with each of the 3 galloyl groups forming one leg of the tripod (figure 1c). These cofactors are used to study the effect of solvent on PEO/cofactor complexes.

2.3 Solvated gallic acid

For the solute (GA) interacting with the solvent (S), the reversible association is:

$$\mathrm{A} + \mathrm{S} \rightleftharpoons \mathrm{A}' \cdot \mathrm{S}' \qquad (1)$$

Equation (1) assumes that the bonds between A and S are stronger than within A·A and S·S, and shows that, when A (GA) and S (H_2O) associate, their structures rearrange to form a more stable complex $A' \cdot S'$ ($GA \cdot (H_2O)_n$). The solvent molecules (H_2O) were positioned manually at different locations around the solute, followed by energy minimization. For more than one water molecule, they were clustered manually followed by energy minimization. These calculations were repeated many times to obtain reliable energy minima within $5\,\mathrm{kcal\,mol^{-1}}$.

The enthalpy of hydration ($\Delta H_{\mathrm{hyd,0\,K}}$) of GA with water was calculated at 0 K:

$$\Delta H^{\mathrm{A'\cdot S'}}_{\mathrm{hyd,0\,K}} = H^{\mathrm{A'\cdot S'}}_{f,\mathrm{0\,K}} - \sum\left(H^{\mathrm{A}}_{f,\mathrm{0\,K}} + H^{\mathrm{S}}_{f,\mathrm{0\,K}}\right) \qquad (2)$$

and then at 298 K, $\Delta G^{\mathrm{A'\cdot S'}}_{\mathrm{298\,K}}$, $\Delta H^{\mathrm{A'\cdot S'}}_{\mathrm{298\,K}}$ and $T\Delta S^{\mathrm{A'\cdot S'}}_{\mathrm{298\,K}}$ from the frequency analysis [42]. Gaussian [38,42] calculates the entropy caused by vibrational, translational, rotational and electronic motions.

2.4 Solvated $(PEO)_6$/TGG complex

For very flexible and asymmetrical molecules such as PEO/TGG complexes, equation (3) is more precise in describing the real situation when PEO and TGG are studied in water. The solute ($(PEO)_6$/TGG) ($A'' \cdot B''$) and solvent $(H_2O)_n$ (S) interact, hence:

$$\mathrm{A}'' \cdot \mathrm{B}'' + \mathrm{S} \rightleftharpoons \mathrm{A}'' \cdot \mathrm{B}'' \cdot \mathrm{S} \qquad (3)$$

To simplify the notation, the subscript in ΔH_{hyd} and superscript in $A'' \cdot B''$ and S' will be omitted in what follows.

The solvation of the $(PEO)_6$/TGG complex was studied using two different approaches [43]: (i) the $(PEO)_6$/TGG was surrounded by sufficient H_2O molecules to give a monolayer: this structure was then minimized by PM3; and (ii) the $(PEO)_6$/TGG was put into a periodic box and molecular dynamics (MD) performed for 7.5 and 75 ps; this structure was then minimized by molecular mechanics (MM). The MD was performed using two sizes of periodic box; (i) $25 \times 20 \times 30\,\mathrm{Å}^3$ having 459 H_2O molecules and (ii) $30.25 \times 30.25 \times 30.25\,\mathrm{Å}^3$ having 906 H_2O molecules [43]. The size of the box has to be about twice the largest dimension (length) of the $(PEO)_6$/TGG complex [43]. The MD calculations were performed with the following heating times 2 ps* and 20 ps**, running times: 3.5 ps* and 35 ps**, cooling times: 2 ps* and 20 ps**, step size: 0.001 ps, starting temperature of 0 K, simulation temperature of 300 K, final temperature of 0 K and temperature step of 1 K (* and ** stands for a total MD time of 7.5 and 75 ps, respectively [43]). After the MD calculations, the resulting $(PEO)_6$/TGG complex structures were used to calculated their PM3 enthalpies of association at 0 K ($\Delta H_{\mathrm{0\,K}}$) [43].

3. Results and discussion

3.1 PEO

The heat of formation of the hexamer of PEO is $H_{f,\mathrm{0\,K}} = -256.71\,\mathrm{kcal\,mol^{-1}}$ [19]. The hexamer ($(PEO)_6$) was used to ensure that the linear length is greater than the model cofactor size to minimize end group effects of CH_3 and OH.

3.2 Gallic acid/$(H_2O)_n$

The heat of formation $H_{f,\mathrm{0\,K}}$ of GA is $-198.24\,\mathrm{kcal\,mol^{-1}}$ (table 1). GA and H_2O associate in many ways at 0 K, as described in table 2 and figure 2. The hydration enthalpy results at 0 K for GA with one H_2O molecule, located at the positions *para* (*p*-OH), *meta* (*m*-OH) and at the carboxylic (–COOH) group, are −3.97, −5.13 and

Table 1. Heats of formation of the cofactors and water (figure 1).

Cofactor	*Conformer*	*$H_{f,0\,K}$ (kcal mol^{-1})*
Gallic acid (GA) [8]		− 198.24
TGG [8]	Tripod	− 670.42
Water		− 53.44*

* For non-clustered single H_2O molecule.

Table 2. Thermochemistry of GA·$(H_2O)_n$ at 0 and 298.15 K.

GA·$(H_2O)_n$ system	$\Delta H_{298\,K}$* (kcal mol^{-1})	$\Delta H_{0\,K}$ (kcal mol^{-1})	*$T\Delta S_{298\,K}$* (kcal mol^{-1})*	$\Delta G_{298\,K}$* (kcal mol^{-1})
GA·*p*-OH·$(H_2O)_1$	− 2.26	− 3.97	− 8.87	+ 6.60
GA·*m*-OH·$(H_2O)_1$	− 3.43	− 5.13	− 8.40	+ 4.97
GA−COOH·$(H_2O)_1$	− 3.54	− 5.95	− 10.23	+ 6.69
[†]GA·$(H_2O)_5$	− 7.09	− 9.27	− 14.39	+ 7.3
[†]GA·$(H_2O)_6$	− 3.77	− 6.32	− 17.18	+ 13.42
GA·$(H_2O)_7$	− 5.01	− 7.81	− 15.07	+ 10.06
[‡]GA·$(H_2O)_{10}$	− 4.90	− 8.76	− 14.11	+ 9.21
GA·$(H_2O)_{40}$	− 8.10	− 12.57	− 22.92	+ 14.81
[¶]GA·$(H_2O)_{43}$	− 8.86	− 17.36	− 38.80	+ 29.93

[*] Scaling factor of 0.9761[41]. [†] The H_2O molecules are all located around the COOH group. [‡] Seven H_2O molecules associated with the COOH group and three associated with the phenolic hydroxyl groups. [¶] Approximately a monolayer of solvent molecules.

-5.95 kcal mol^{-1}, respectively. These results agree qualitatively with those of Madhan *et al.* [31], who used the *ab initio* HF/6-31G* method, to give GA·$(H_2O)_1$ binding energies of -2.16, -3.67 and -7.4 kcal mol^{-1} for GA·*p*-OH·$(H_2O)_1$, GA·*m*-OH·$(H_2O)_1$ and GA–COOH·$(H_2O)_1$, respectively. However, the thermochemistry analysis at 298.15 K shows almost identical results for (*m*-OH) and –COOH (table 2). Even though, the theoretical hydration enthalpies in table 2 are in the range of the experimental value, -10.78 kcal mol^{-1}, reported by Forteza *et al.* [37], the thermochemistry analyses showed that GA·$(H_2O)_n$ systems do not form at room temperature because $\Delta G \geq 0$. The present study like that of Madhan *et al.* [31] is a model treatment. In reality, GA will be ionised

$$\mathrm{COOH} + \mathrm{H_2O} \rightleftharpoons \mathrm{COO^-} + \mathrm{H_3O^+}$$

at a pH of 6.8, the pH that was used in our experiments [44] and typical of papermaking conditions. It could

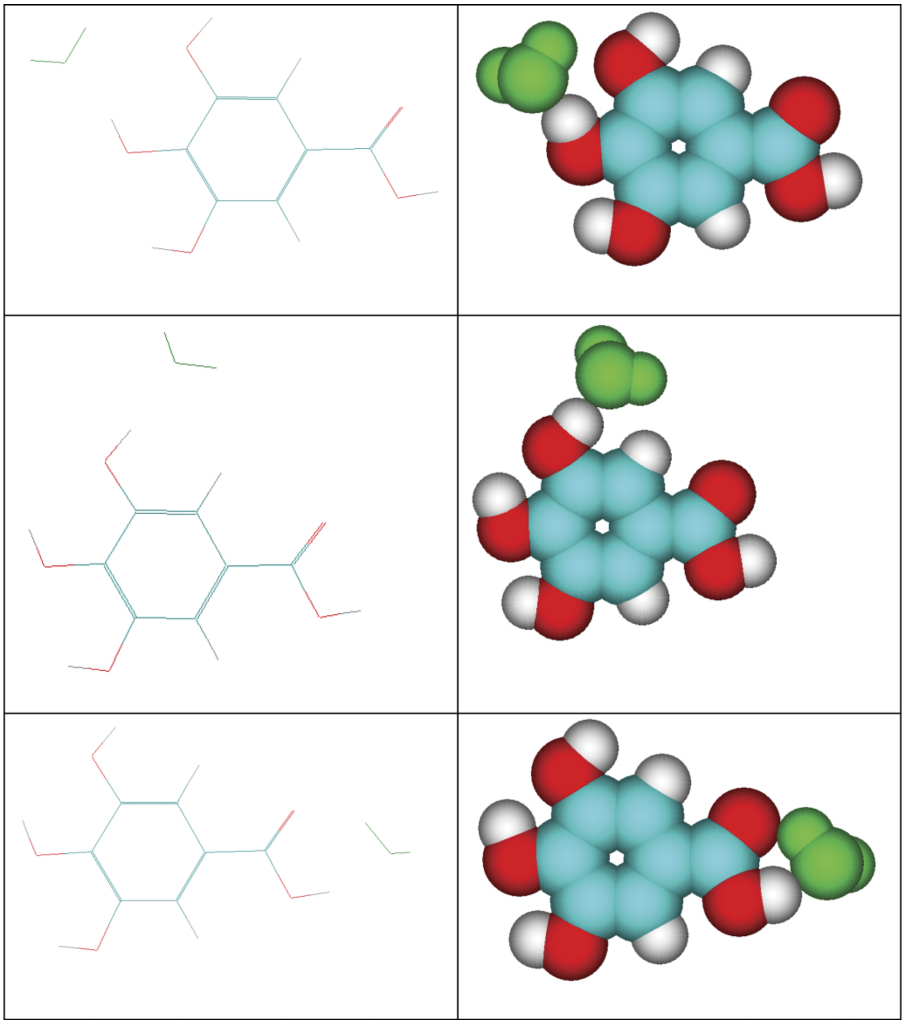

Figure 2. Stick diagram (left) and their corresponding overlapping spheres model for GA·$(H_2O)_1$: (*p*–OH) (top), *m*–OH (centre) and –COOH (bottom).

be considered that at a pH ≈ 2, the equilibrium would be completely towards the COOH.

Figure 2 shows the most stable conformations obtained for the GA·$(H_2O)_1$ systems, but at 0 K many other minima exist with slightly less stable enthalpies of association, within $3\,\text{kcal mol}^{-1}$. Figure 3 shows the most stable conformation found for larger systems, GA·$(H_2O)_5$ and GA·$(H_2O)_6$, in which the H_2O molecules are clustered around the COOH group. All other calculations gave hydration energies which were much higher, and much less stable, for the $(H_2O)_6$ clustered around the phenolic hydroxyl groups or on both sides of the benzene ring, agreeing with the ideas of Muller-Dethlefs and Hobza [16]. Among the several different water hexamers, the cage form is the most stable in the gas phase [46].

In the present paper, the most stable system was found to be seven H_2O molecules clustered around the hydrophilic COOH group, and three on the hydroxyl groups of GA·$(H_2O)_{10}$ (figure 3, bottom). Interestingly, GA·$(H_2O)_7$ and GA·$(H_2O)_{10}$ show ΔG and $T\Delta S$ to be smaller. These are both gas phase and 298 K calculations.

It now became interesting to see whether adding many more H_2O molecules would allow the entropy change ΔS to be less important and make ΔG negative. The number of H_2O molecules was chosen to form a monolayer around GA, which required about 43 H_2O molecules (equation (4) and figure 4). GA·$(H_2O)_{43}$, not considering GA dissociation, readily hydrates at 0 K:

$$\begin{array}{ccc} \text{GA} + (\text{H}_2\text{O})_{43} & \rightleftharpoons & \text{GA}\cdot(\text{H}_2\text{O})_{43} \\ -198.24 + -2551.66 & & -2767.26 \end{array} \tag{4}$$

since the complex ($H_{f,0\,\text{K}} = -2767.26\,\text{kcal mol}^{-1}$) is more stable than the sum of the reactants ($\Sigma(H_{f,0\,\text{K}}^{\text{GA}} + H_{f,0\,\text{K}}^{(\text{H}_2\text{O})_{43}}) = -2749.90\,\text{kcal mol}^{-1}$). From equation (4),

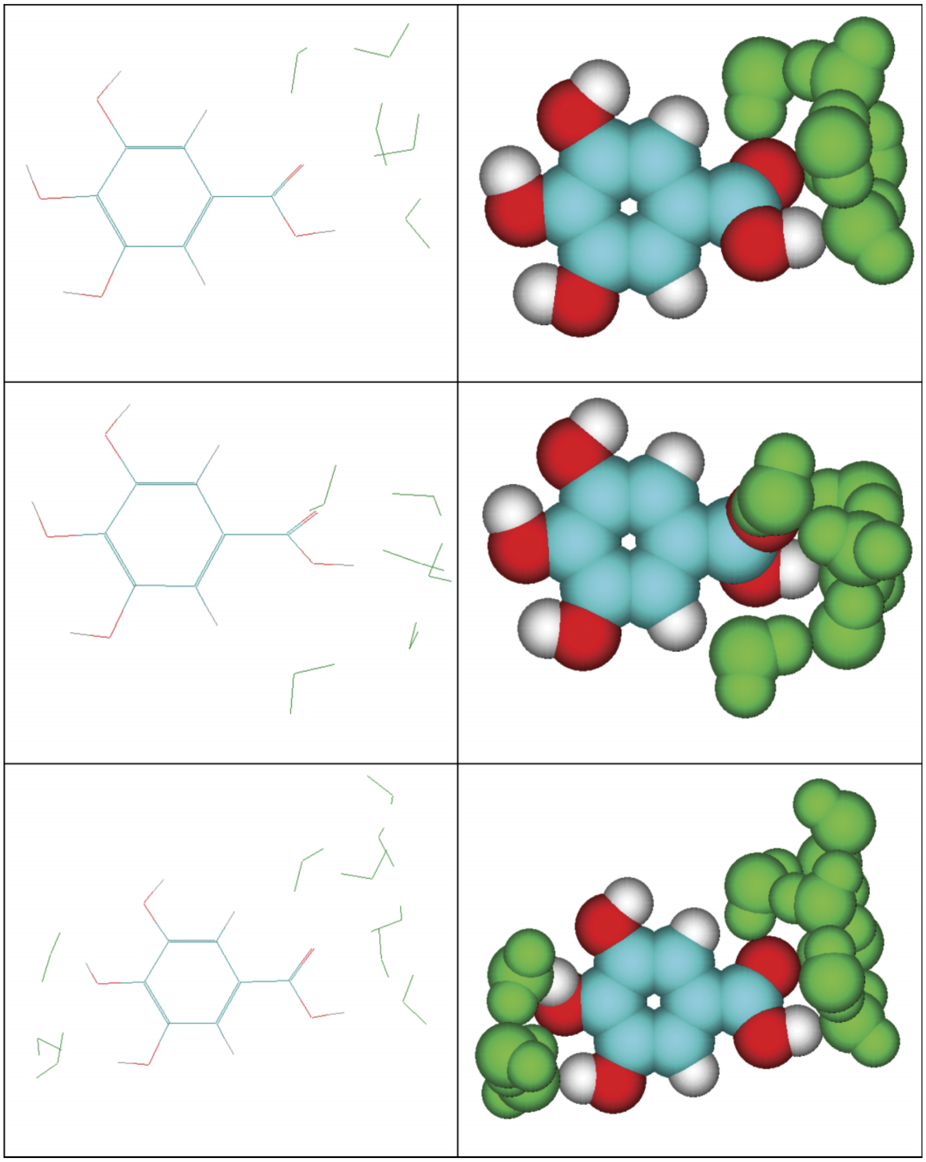

Figure 3. Stick diagram of GA·$(H_2O)_5$ (top left), GA·$(H_2O)_6$ (centre left) and GA·$(H_2O)_{10}$ (bottom left) and their corresponding overlapping spheres model (right).

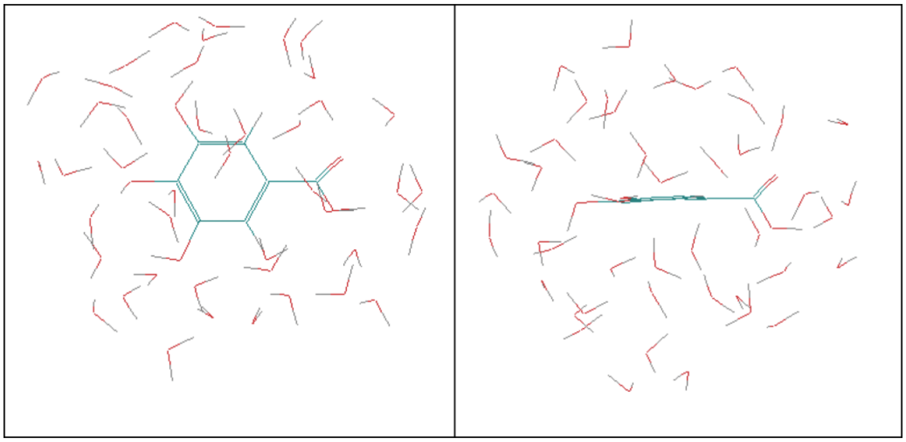

Figure 4. Top view and side view of the first shell of 43 water molecules around gallic acid (GA·$(H_2O)_{43}$).

the hydration enthalpy of GA·$(H_2O)_{43}$ is -17.36 kcal mol^{-1} at 0 K.

Remember that numerous conformations exist for each of these systems, within about 5 kcal mol^{-1}; nevertheless those shown in figures 2–4 are the global minima for these systems.

The position of the H_2O molecules around the hydrophilic and hydrophobic part of GA in figure 4 is interesting. The H_2O molecules form a sphere around the hydrophobic part without any direct contact. However, the H_2O molecules around the hydrophilic part are closer to the solute and more regularly oriented. This correlates well with results of Malardier *et al.* [16] obtained for the water conformation around styrene–maleic anhydride, where the hydrophilic interactions were found to be direct and long range, while the hydrophobic interactions were found to be indirect and short range.

Increasing the hydration number (n_h) increases the free energy ($\Delta G_{298\,K}$), the hydration enthalpy ($\Delta H_{298\,K}$) and entropy ($T\Delta S_{298\,K}$) on an absolute scale (table 2) and the change in enthalpy of hydration (figure 5). The interpretation of figure 5 is interesting because when $n_h \leq 10$, the hydration enthalpy must be a function of the hydrophilic interactions between H_2O and COOH or OH (figures 2 and 3), whereas, from $n_h = 40$ to 43, it must be a function of both hydrophilic and hydrophobic interactions (figure 4). Theoretically, the slope reflecting the hydrophilic interactions must be steeper than that for the hydrophobic, and the combined interactions. However, there is another parameter involved when n_h is larger than one; it is the binding energy within the solvent S·S, which contributes to lower the change in enthalpy. The binding energy increases from $n_h = 1$ until bulk water is reached, when the relative total energy per mole of H_2O molecules becomes constant.

Figure 6 shows that a change in the enthalpy of hydration ΔH_h is accompanied by a change in entropy of hydration ΔS_h. As the number of H_2O molecules increases, the slope of ΔH_h against ΔS_h tends to plateau out towards $n = 40$ and 43. This correlates with the results obtained when two molecules associate and change their conformation to form the most stable complex [47–49].

From a thermodynamic study of GA and water, the dissociation constant of GA at 25°C was calculated to be $(3.7 \pm 0.1) \times 10^{-5}$ [50]; the speed of sound and the density were used to yield a hydration number of ≈ 6 for

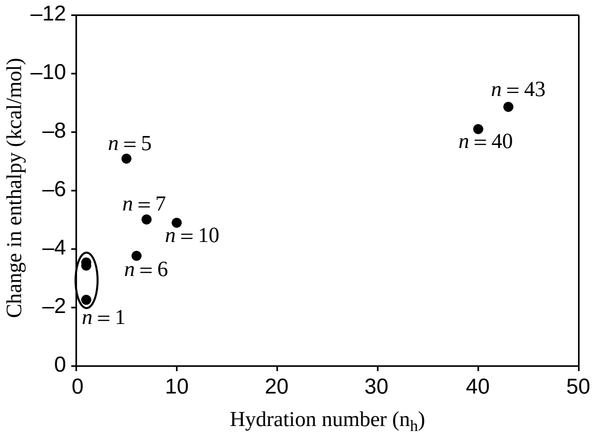

Figure 5. Change in enthalpy of hydration ΔH_h of gallic acid at 298.15 K as a function of the hydration number n_h for (GA·$(H_2O)_n$).

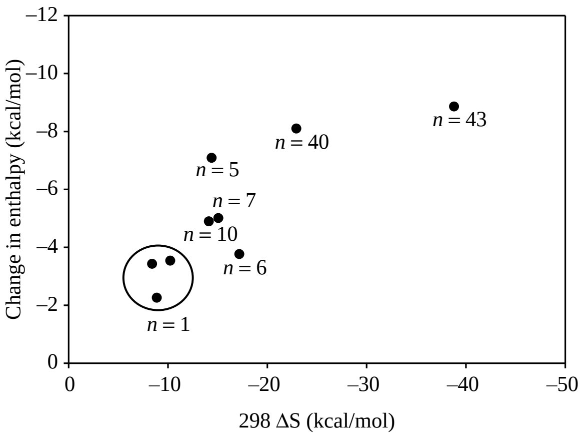

Figure 6. The change in the calculated enthalpy of hydration ΔH_h, as a function of the calculated entropy change ΔS_h at 298.15 K, between gallic acid and water (n equals the number of H_2O molecules).

the hydration shell [50]. The hydration number was constant from 0.01 to 0.055 M aqueous solutions of GA [50]. This is different from our calculation which shows that it takes about 43 H_2O molecules to form a monolayer around GA (figure 4). It is difficult to conceive of a hydration shell for GA containing only 6 H_2O molecules. Martinez *et al.* [50] reported that "these low values for the hydration number may be explained by the weak hydrophobic character and the small size of GA". The present calculations suggest that this is an incorrect interpretation; the 6 H_2O molecules observed by them must be the ones associated with the hydrophilic part of GA (figure 3, centre), whereas H_2O molecules near the hydrophobic part of GA are not detected.

3.3 *(PEO)$_6$/TGG: Gas phase*

The TGG-tripod conformer [8] was used for the calculations, and for simplicity, it will be called simply TGG. Equation (5) shows that $(PEO)_6$/TGG readily complexes at 0 K, (figure 7, left):

$$\begin{array}{ccc} (\mathrm{PEO})_6 + \mathrm{TGG} & \rightleftharpoons & (\mathrm{PEO})_6/\mathrm{TGG} \\ -256.71 + -670.42 & & -944.49 \end{array} \qquad (5)$$

because the complex ($\Delta H_{f,0\,\mathrm{K}} = -944.49\,\mathrm{kcal\,mol^{-1}}$) is more stable than the sum of the reactants ($\Sigma(H_{f,0\,\mathrm{K}}^{(\mathrm{PEO})_6} + H_{f,0\,\mathrm{K}}^{\mathrm{TGG}}) = -927.13\,\mathrm{kcal\,mol^{-1}}$). The enthalpy of association ($\Delta H_{0\,\mathrm{K}}$), in the gas phase is, therefore, -17.36 $\mathrm{kcal\,mol^{-1}}$.

3.4 *TGG/(PEO)$_6$/(H$_2$O)$_n$: Solvated*

When H_2O molecules are either surrounding the TGG/$(PEO)_6$ or the complex is put in a water continuum in a periodic box, then as equation (6) shows $(PEO)_6$/TGG/$(H_2O)_{122}$ will not form (figure 7):

$$\begin{array}{cc} (\mathrm{PEO})_6 + \mathrm{TGG} + (\mathrm{H_2O})_{122} & \rightleftharpoons (\mathrm{PEO})_6/\mathrm{TGG}/(\mathrm{H_2O})_{122} \\ -256.71 + -670.42 + -7328.64 & -8174.92 \end{array} \qquad (6)$$

because the total enthalpy of the system at 0 K ($\Delta H_{f,0\,\mathrm{K}} = -8174.92\,\mathrm{kcal\,mol^{-1}}$), is less stable than the sum of the reactants $\Sigma(H_{f,0\mathrm{K}}^{(\mathrm{PEO})_6} + H_{f,0\mathrm{K}}^{\mathrm{TGG}} + H_{f,0\mathrm{K}}^{(\mathrm{H_2O})_{122}}) = -8255.77\mathrm{kcalmol^{-1}}$ and consequently $\Delta H_{0\,\mathrm{K}}$ is $+80.85\,\mathrm{kcal\,mol^{-1}}$. These results show that the complex is thermodynamically unstable.

However, because there is a possibility that a MO calculation is perhaps not adequate, this complex was further studied using MD followed by MM geometry optimization. This shows the effect of water on the $(PEO)_6$/TGG conformation and the energy balance of this system was determined (figure 8 and tables 3, 4).

MD simulations show that the $(PEO)_6$/TGG complex separates as the MD calculation time increases in the heating stage. In other words, it will not form in aqueous solution, which agrees with the MO calculations and which also agrees with the experimental results obtained with PEO and corilagin, a very similar cofactor [43–45].

Table 3 shows that the dynamic simulation time should ideally have been extended further, since the system became more stable, with a lower energy, going from 7.5 to 75 ps (≅ 5 weeks of calculation time). Consequently, the optimum MD time is unknown; nevertheless the trend shows clearly that $(PEO)_6$ and TGG are separating from each other and their conformations are less stable (figure 8). Moreover, the smallest distance left after 75 ps between PEO–CH···H–TGG is 2.61 Å (figure 8, bottom right). Garcia and Stiller [51] reported that the mean residence time (MRT) of H_2O molecules in the first hydration shell of atoms, or groups, range from a few picoseconds for polar and non-polar groups to over 50 ps for charged groups of biomolecules. They [51] also reported that the average lifetime of a hydrogen bond in proteins is around 2 ps. They generalized their results

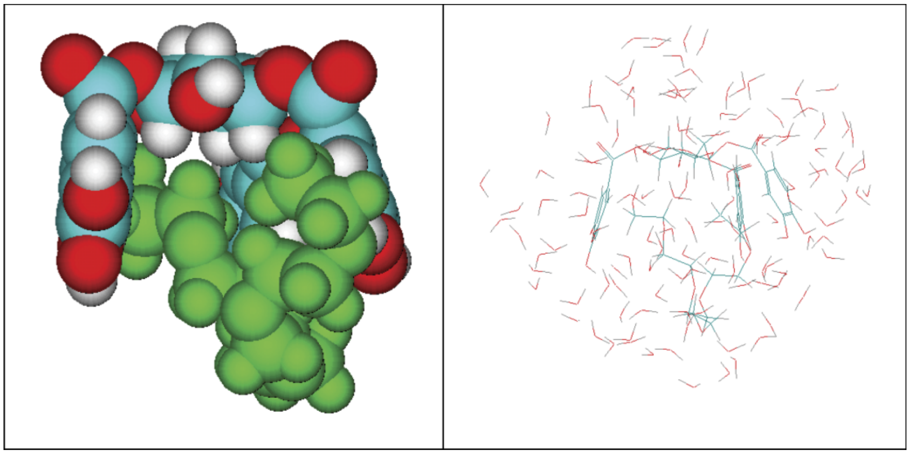

Figure 7. Gas phase $(PEO)_6$/TGG complex (left) and solvated $(PEO)_6$/TGG/$(H_2O)_{122}$ system (right) showing the effect of solvent on $(PEO)_6$/TGG conformation.

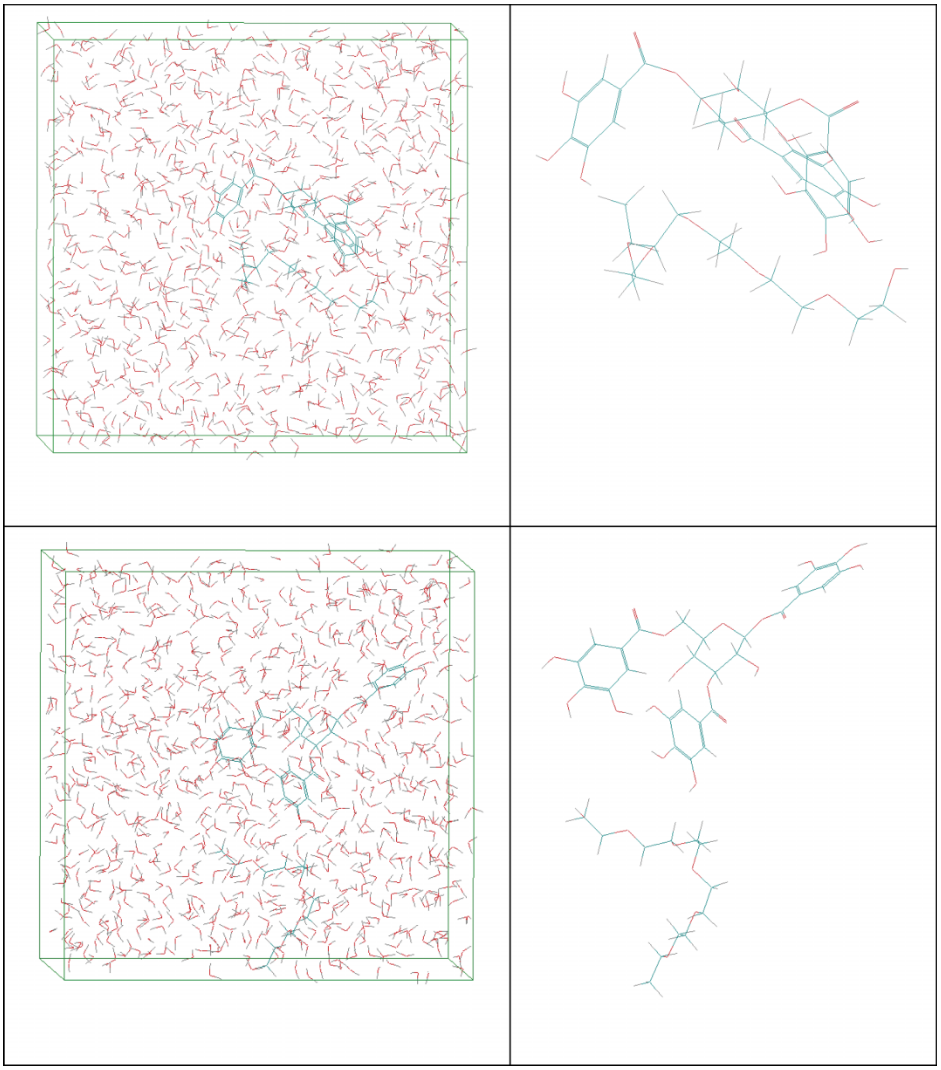

Figure 8. Solvated $(PEO)_6/TGG/(H_2O)_{906}$ system showing the effect of solvent on $(PEO)_6/TGG$ conformation after molecular dynamics (MD) simulations of 7.5 ps (top) and 75 ps (bottom) followed by molecular mechanics (MM). The figures on the right show the $(PEO)_6$ and TGG conformation after the MD–MM calculations.

by ranking the MRT in the order: $\tau_{\text{charged}} > \tau_{\text{polar}} > \tau_{\text{nonpolar}} \approx \tau_{\text{bulk-water}}$ [51]. Impey *et al.* [52] reported a residence time $\tau_{\text{ion}}^{\text{S}}$ of 4.8 ps for potassium (K^+) at 274 K, where $\tau_{\text{ion}}^{\text{S}}$ is the characteristic time over which the H_2O molecules in the first coordination shell exchange identity with molecules in the bulk, and hence for any correlation, between the ion and any particular water molecule, to be lost. This emphasizes that our MD calculations are valid and extending the time would have resulted in a confirmation in the obvious trend.

Table 3. Total energy of $(PEO)_6/TGG/(H_2O)_n$ system as a function MD calculation time.

System	*Total energy (kcal mol^{-1})*		
*MD–MM**	*MD = 7.5 ps*	*MD = 75 ps*	*Difference*
$(PEO)_6/TGG/(H_2O)_{459}$	− 1251.5	− 1328.08	− 76.58
$(PEO)_6/TGG/(H_2O)_{906}$	− 2635.11	− 2737.08	− 101.97

* MD–MM: Molecular dynamics (MD) followed by molecular mechanics (MM).

Table 4 shows the enthalpy balance for the gas phase $(PEO)_6/TGG$ and solvated complexes, but excludes the enthalpy contribution from water. This approach selectively points to the effect of solvent on the solute conformation and the enthalpy of association.

Interestingly, for PM3 calculations the enthalpy of formation for solvated $(PEO)_6$, $-258.95\,\text{kcal mol}^{-1}$, is more stable than the gas phase enthalpy of formation of $(PEO)_6$, $-256.71\,\text{kcal mol}^{-1}$ (table 4). This is because $(PEO)_6$ has an intermediate structure between crystalline [53], with the ether oxygens inside the helical molecule, and a more stable conformer with the oxygens outside (figure 9). This structure is probably favoured in aqueous solution because the H_2O molecules can more easily hydrogen bond with the PEO ether oxygens. This conformation is probably the reason why PEO is soluble in water, whereas poly(methylene oxide) and poly(propylene oxide) are not. However, TGG is destabilized by the solvent which decreases the enthalpy of association ($\Delta H_{0\,\text{K}}$) from -17.36 to $-6.91\,\text{kcal mol}^{-1}$ (table 4).

Table 4. Enthalpy balance for gas phase and solvated PEO/TGG systems at 0 K.

Computing method	*$(PEO)_6$* *$\Delta H_{f,0\,K}$ (kcal/mol)*	*TGG* *$\Delta H_{f,0\,K}$ (kcal/mol)*	*$(PEO)_6$/TGG* *$\Delta H_{f,0\,K}$ (kcal/mol)*	*$\Delta H_{0\,K}$* *(kcal/mol)*
PM3 (gas phase)	− 256.71	− 670.42	− 944.49	− 17.36
PM3 (solvated)*	− 258.95	− 657.98	− 923.74	− 6.91
MD7.5psMM†	− 238.70	− 573.06	− 818.13	− 6.37
MD75psMM†	− 236.85	− 579.50	− 817.23	− 0.88

* $(H_2O)_{122}$. † $(H_2O)_{906}$.

The MD calculations drastically changed the conformation of $(PEO)_6$ and TGG (figure 8), and consequently decreased further the enthalpy of association (table 4). Even though the energy balance was only performed at 0 K, for computational time constraints, by analogy to previous results [9], it can be concluded that $(PEO)_6$/TGG will not associate at room temperature because $\Delta G \geq 0$.

3.5 *Effect of the number of H_2O molecules on the relative total energy per mole of H_2O molecules*

Figure 10, which was constructed using the results of the PM3 semiempirical method, shows that the relative total energy per mole of H_2O molecules changes as a function of the number of H_2O molecules, and therefore, differs from one system to another $(GA{\cdot}(H_2O)_n)$. The trend shown is consistent with the results of Upadhyay *et al.* [46], obtained with *ab initio* calculations, who observed the onset of a plateau at about 10 H_2O molecules.

The relative total energy per mole of water becomes more negative as the number of H_2O molecules increases, showing that hydrogen bonding between the H_2O makes the total H_2O system more stable. This observation is critical when analysing systems with different numbers of H_2O molecules. To perform an energy balance, for H_2O molecules which are clustered, the relative total energy of H_2O in the cluster must be recalculated for each H_2O system, otherwise a significant error will occur. For example, when comparing two systems having 40 and 70 H_2O molecules, where the relative total energy per mole of molecules is -59.07 and -60.07 kcal mol^{-1}, respectively (figure 10), ignoring the change in energy of each H_2O in each cluster, would give an error of -30 kcal mol^{-1}. Figure 10 shows a distinct change in the rate of change of the relative energy per H_2O at 10 H_2O molecules; after this a slower varying plateau is observed to and beyond 120 H_2O molecules.

Bondebey *et al.* [54] using (FT-ICR) mass spectrometry and B3LYP describe a variety of reactions and processes in clusters of up to 100 H_2O molecules and found they behaved like bulk H_2O solutions. However, Bondebey *et al.* [54] concluded that the bulk behaviour of H_2O is regularly exhibited by clusters containing on the order of 10 H_2O molecules, in agreement with the present PM3 results, and those of Stace [55] from gas phase thermochemistry.

4. Conclusions

The results of the PM3 calculations on the interactions of water with GA show that the H_2O molecules form a sphere around the hydrophobic part of GA, without any direct contact. The H_2O molecules around the hydrophilic part are closer to the solute (GA) and form strong directional bonds. The total number of H_2O molecules to cover both the hydrophobic and hydrophilic regions of GA is about 43, forming a monolayer around GA. The hydrophilic COOH region of GA has 5 H_2O molecules associated with it. This can be compared to the calculations of water clusters by Upadhyay *et al.* which gave the most stable cluster as six H_2O in a cage structure. In our work, one

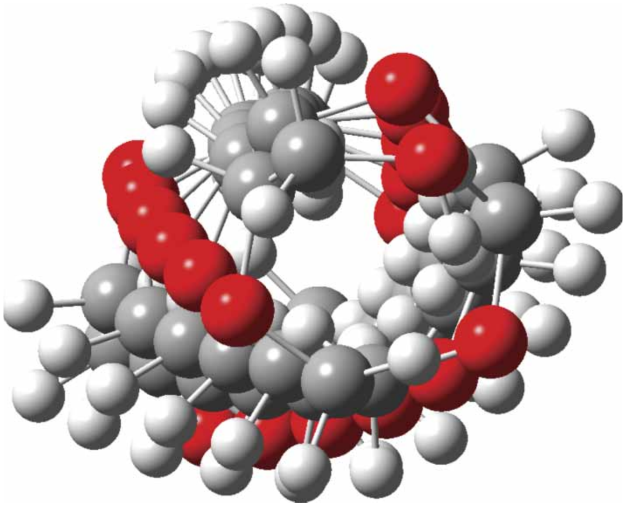

Figure 9. Molecular conformation of poly(ethylene oxide) (PEO_{18}) with the ether oxygens outside.

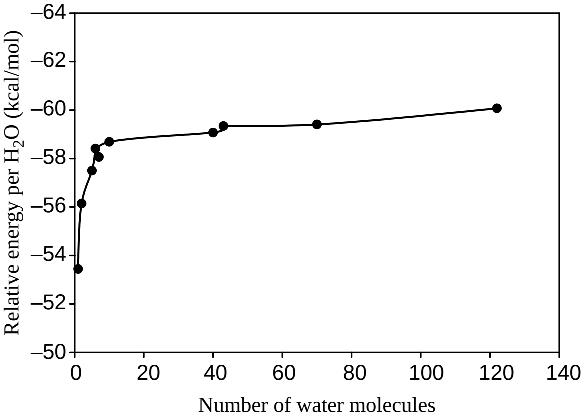

Figure 10. Relative total energy per mole of water molecules at 0 K as a function of the number of H_2O molecules.

of the H_2O molecules is replaced by the COOH group of GA. A hydration number of ≈ 6 was found for the hydration shell of GA by Martinez *et al.* It is possible that their experimental methods only consider the molecules associated with the hydrophilic groups.

The present PM3, MM and MD calculations show that $(PEO)_6$/TGG complexes will not form in aqueous solution, which agrees with the experimental results in pure water in the absence of salt obtained with PEO and corilagin, a very similar cofactor. It is possible that a $(PEO)_6$ conformer, with the oxygens outside, is favoured in aqueous solution, because the H_2O molecules can more easily hydrogen bond with the PEO ether oxygen's.

A distinct change in the rate of change of the relative total energy per H_2O occurs at 10 H_2O molecules: beyond 10 H_2O molecules a slow varying plateau is observed to and beyond 120 H_2O molecules. This information is critical when calculating the enthalpy of association of a solvated molecular complex.

Acknowledgements

This Research was supported by the NSERC (Canada). The funding awarded by an Industrial Research Chair (NSERC) and Paprican is great fully acknowledged.

References

[1] T. Lindström, G. Glad-Normark. Flocculation of latex and cellulose dispersions by means of transient polymer networks. *Colloids Surf.*, **8**, 337 (1984).

[2] H. Xiao, R. Pelton, A. Hamielec. Retention mechanisms for two-component systems based on phenolic resins and PEO or new PEO-copolymer retention aids. *J. Pulp Paper Sci.*, **22**(12), J475 (1996).

[3] T.G.M. van de Ven, B. Alince. Association-induced polymer bridging: new insights into the retention of fillers with PEO. *J. Pulp Paper Sci.*, **22**(7), J257 (1996).

[4] T.G.M. van de Ven, B. Alince. Heteroflocculation by asymmetric polymer bridging. *J. Colloid Interface Sci.*, **181**, 73 (1996).

[5] P. Englezos, P. Pang. Kinetics of the flocculation of clay particles by polyethylene oxide (PEO) at temperatures above the PEO–water cloud point temperature. *Nordic Pulp Paper Res. J.*, **15**(5), 387 (2000).

[6] C. Lu. Mechanisms of filler flocculation with PEO/cofactor dual-component Flocculants, PhD Thesis, McMaster University, Ontario, Canada, April 2003.

[7] S. Goto, R. Pelton. The influence of phenolic cofactors on the properties of calcium cabonate flocs formed with PEO. *Colloids Surf. A: Physicochem. Eng. Aspects*, **155**, 231 (1999).

[8] R. Gaudreault, M.A. Whitehead, T.G.M. van de Ven. Molecular modeling of poly(ethylene oxide) model cofactors; 1,3,6-tri-*O*-galloyl-β-D-glucose and corilagin. *J. Mol. Model.*, **8**, 73 (2002).

[9] R. Gaudreault, M-A. Whitehead, T.G.M. van de Ven. Molecular orbital studies of gas phase interactions between complex molecules, (submitted to J. Phys. Chem. A.)

[10] K.R. Stack, L.A. Dunn, N.K. Roberts. Study of the interaction between poly(ethylene oxide) and phenol–formaldehyde resin. *Colloids Surf.*, **61**, 205 (1991).

[11] R. Pelton, H. Xiao, M.A. Brook, A. Hamielec. Flocculation of polystyrene latex with mixtures of poly(*p*-vinylphenol) and poly(ethylene oxide). *Langmuir*, **12**, 5756 (1996).

[12] C.J. Cramer, D.G. Truhlar. PM3–SM3: a general parameterization for including aqueous solvation effects in the PM3 molecular model. *J. Comp. Chem.*, **13**(9), 1089 (1992).

[13] F.M. Floris, J.M. Martìnez. Preferential solvation of Ca^{2+} in aqueous solutions containing ammonia: A molecular dynamics study. *J. Chem. Phys.*, **116**(13), 5460 (2002).

[14] J. Chandrasekhar, S. Shariffskul, W.L. Jorgensen. QM/MM simulations for Diels–Alder reactions in water: contributions of enhanced hydrogen bonding at the trasition state to the solvent effect. *J. Phys. Chem. B*, **106**, 8078 (2002).

[15] J. Gao. Hybrid quantum and molecular mechanical simulations: an alternative avenue to solvent effects in organic chemistry. *Acc. Chem. Res.*, **29**, 298 (1996).

[16] C. Malardier-Jugroot, T.G.M. van de Ven, M.A. Whitehead. Study of the water conformation around hydrophilic and hydrophobic parts of styrene–maleic anhydride. *J. Mol. Struct. (Theochem.)*, **679**, 171 (2004).

[17] K. Müller-Dethlefs, P. Hobza. Noncovalent interactions: a challenge for experiment and theory. *Chem. Rev.*, **100**, 143 (2000).

[18] T.G.M. van de Ven, *Colloidal Hydrodynamics*, Copyright 1989 by Academic Press Limited, Chapter 5, pp. 359–363.

[19] J. Florián, A. Warshel. Calculations of hydration entropies of hydrophobic, polar, and ionic solutes in the framework of the langevin dipoles solvation model. *J. Phys. Chem. B*, **103**, 10282 (1999).

[20] A. Warshel. Calculations of chemical processes in solutions. *J. Phys. Chem.*, **83**, 1640 (1979).

[21] A.A. Rashin, L. Young, I.A. Topol. Quantitative evaluation of hydration thermodynamics with a continuum model. *Biophys. Chem.*, **51**, 359 (1994).

[22] T. Steiner. The whole palette of hydrogen bonds. *Angew. Chem. Int. Ed.*, **41**, 48 (2002).

[23] T. Steiner, G.R. Desiraju. Distinction between the weak hydrogen bond and the van der Waals interaction. *Chem. Commun.*, 891 (1998).

[24] T. van Mourik, F.B. van Duijneveldt. Ab initio calculations on the C–H ...O hydrogen-bonded systems CH_4–H_2O, CH_3NH_2–H_2O and CH_3NH_3–H_2O. *J. Mol. Struct.: Theochem.*, **341**, 63 (1995).

[25] T. Steiner, W. Saenger. Geometry of the C–H...O hydrogen bonds in carbohydrate crystal structures. Analysis of neutron diffraction data. *J. Am. Chem. Soc.*, **114**, 10146 (1992).

[26] X. Yan, S. Wang, M. Hodošček, G.W.A. Milne. Prediction of geometries and interaction energies of complexes formed by small molecules using semiempirical and ab initio methods. *J. Mol. Struct.: Theochem.*, **309**, 279 (1994).

[27] J.C. Lee Jr., E. Peris, A.L. Rheingold, R.H. Crabtree. An unusual type of H...H interaction: Ir–H...H–O and Ir–H...H–N hydrogen bonding and its involvement in σ-bond metathesis. *J. Am. Chem. Soc.*, **116**, 11014 (1994).

[28] W.T. Klooster, T.F. Koetzle, Per E.M. Siegbahn, T.B. Richardson, R.H. Crabtree. Study of the N–H...H–B dihydrogen bond including the crystal structure of BH3NH3 by neutron diffraction. *J. Am. Chem. Soc.*, **121**(27), 6337 (1999).

[29] P. Hobza, V. Špirko, H.L. Selzle, E.W. Schlag. Anti-hydrogen bond in the benzene dimer and other carbon proton donor complexes. *J. Phys. Chem. A*, **102**, 2501 (1998).

[30] P. Hobza, V. Špirko, Z. Havlas, K. Buchhold, B. Reimann, H-D. Barth, B. Brutschy. Anti-hydrogen bond between chloroform and fluorobenzene. *Chem. Phys. Lett.*, **299**, 180 (1999).

[31] B. Madhan, P. Thanikaivelan, V. Subramanian, J. Raghava Rao, Balachandran Unni Nair, T. Ramasami. Molecular mechanics and dynamic studies on the interaction of gallic acid with collagen-like peptides. *Chem. Phys. Lett.*, **346**, 334 (2001).

[32] M.D. Benoit, D.C. Clary. Quantum simulation of phenol–water clusters. *J. Phys. Chem. A*, **104**, 5590 (2000).

[33] H.H.Y. Tsui, T. van Mourik. Ab initio calculations on phenol–water. *Chem. Phys. Lett.*, **350**, 565 (2001).

[34] A. Courty, M. Mons, I. Dimicoli, F. Piuzzi, V. Brenner, P. Millié. Ionization energetics, and geometry of the phenol–S complexes (S=H_2O, CH_3OH, and CH_3OCH_3). *J. Phys. Chem.*, **102**, 4890 (1998).

[35] G. Hummer, S. Garde, A.E. García, L.R. Pratt. New perspectives on hydrophobic effects. *Chem. Phys.*, **258**, 349 (2000).

[36] A. Krilov, A. Holmgren, R. Gref, L.O. Ohman. Effects of gallic acid on metals: an ft-ir study of complexes between gallic acid and sawblade steel. *Holzforschung*, **47**, 239 (1993).

[37] R. Forteza, A. Caro, J.M. Estela, V. Cerdá. Calculation and refinement of thermodynamic parameters from thermometric titrations. II. The neutralization enthalpies of phenols in hydro-alcoholic media. *Thermochim. Acta*, **268**, 105 (1995).

[38] M.J. Frisch, G.W. Trucks, H.B. Schlegel, G.E. Scuseria, M.A. Robb, J.R. Cheeseman, V.G. Zakrzewski, J.A. Montgomery Jr., R.E. Stratmann, J.C. Burant, S. Dapprich, J.M. Millam, A.D. Daniels,

K.N. Kudin, M.C. Strain, Ö. Farkas, T. Tomasi, V. Barone, M. Cossi, R. Cammi, B. Mennucci, C. Pomelli, C. Adamo, C.S. Clifford, J. Ochterski, G.A. Petersson, P.Y. Ayala, Q. Cui, K. Morokuma, P. Salvador, J.J. Dannenberg, D.K. Malick, A.D. Rabuck, K. Raghavachari, J.B. Foresman, J. Cioslowski, J.V. Ortiz, A.G. Baboul, B.B. Stefanov, G. Liu, A. Liashenko, P. Piskorz, I. Komáromi, R. Gomperts, R.L. Martin, D.J. Fox, T. Keith, M.A. Al-Laham, C.Y. Peng, A. Nanayakkara, M. Challacombe, P.M.W. Gill, B. Johnson, W. Chen, M.W. Wong, J.L. Andres, C. Gonzalez, M. Head-Gordon, E.S. Replogle, J.A. Pople. Gaussian 98, Gaussian, Inc., Pittsburgh, PA (1998).

[39] J.J.P. Stewart. Optimization of parameters for semiempirical methods I. Method. *J. Comp. Chem.*, **10**(2), 209 (1989).

[40] J.J.P. Stewart. Optimization of parameters for semiempirical methods II. applications. *J. Comp. Chem*, **10**(2), 221 (1989).

[41] A.P. Scott, L. Radom. Harmonic vibrational frequencies: an evaluation of Hartree-Fock, Moller-Plesset, quadratic configuration interaction, density functional theory, and semiempirical scale factors. *J. Phys. Chem.*, **100**, 16502 (1996).

[42] J.W. Ochterski. *Thermochemistry in Gaussian 2000, Gaussian inc*, June 2, 1–19 (2000).

[43] R. Gaudreault. Mechanisms of floculation with poly(ethylene oxide) and novel cofactors: theory and experiment, PhD Thesis, Dept. of Chem., MGill University, Montreal, Canada, December 2003.

[44] R. Gaudreault, M-A. Whitehead, T.G.M. van de Ven. Mechanisms of flocculation with poly(ethylene oxide) and novel cofactors. *Physicochem Eng. Aspects*, **268**.

[45] R. Gaudreault, M-A. Whitehead, T.G.M. van de Ven. Mechanisms of flocculation of microcrystalline cellulose by poly(ethylene oxide) and cofactor corilagin, Fundamental Research Symposium, Robinson College, Cambridge, England, September 11–16 (2005).

[46] D.M. Upadhyay, M.K. Shukla, P.C. Mishra. An *ab initio* study of water clusters in gas phase and bulk aqueous media: $(H_2O)_n$, $n = 1–12$. *Int. J. Quantum Chem.*, **81**, 90 (2001).

[47] M.S. Searle, M.S. Westwell, D.H. Williams. Application of a generalised enthalpy–entropy relationship to binding co-operativity and weak association in solution. *J. Chem. Soc. Perkin Trans.*, **2**, 141 (1995).

[48] M.S. Westwell, M.S. Searle, J. Klein, D.H. Williams. Successful predictions of the residual motion of weakly associated species as a function of the bonding between them. *J. Phys. Chem.*, **100**, 16000 (1996).

[49] D.H. Wiliams, M.S. Westwell. Aspects of weak interactions. *Chem. Soc. Rev.*, **27**, 57 (1998).

[50] N. Martinez, E. Junquera, E. Aicart. Ultrasonic, density, and potentiometric characterization of the interaction of gentisic and gallic acid with an apolar cavity in aqueous solutions. *Phys. Chem. Chem. Phys.*, **1**, 4811 (1999).

[51] A.E. Garcia, L. Stiller. Computation of the mean residence time of water in the hydration shells of biomolecules. *J. Comp. Chem.*, **14**(11), 1396 (1993).

[52] R.W. Impey, P.A. Madden, I.R. McDonnald. Hydration and mobility of ions in solution. *J. Phys. Chem.*, **87**, 5071 (1983).

[53] Y. Takahashi, H. Tadokoro. Structural studies of polyethers, $(-(CH_2)_m-O-)_n$. X. Crystal structure of poly(ethylene oxide). *Macromolecules*, **6**(5), 672 (1973).

[54] V.E. Bondybey, M.K. Beyer. How many water molecules make a solution? *Int. Rev. Phys. Chem.*, **21**(2), 277 (2002).

[55] A. Stace. Cluster solutions. *Science*, **294**, 1292 (2001).